



Published in final edited form as:

*J Biol Chem.* 2000 May 12; 275(19): 14408–14414.

## Nitrogen Catabolite Repression of *DAL80* Expression Depends on the Relative Levels of Gat1p and Ure2p Production in *Saccharomyces cerevisiae*\*

Thomas S. Cunningham, Roopa Andhare, and Terrance G. Cooper<sup>‡</sup>

Department of Microbiology and Immunology, University of Tennessee, Memphis, Tennessee 38163

### Abstract

GATA family activators (Gln3p and Gat1p) and repressors (Dal80p and Deh1p) regulate nitrogen catabolite repression (NCR)-sensitive transcription in *Saccharomyces cerevisiae* presumably via their competitive binding to the GATA sequences upstream of NCR-sensitive genes. Ure2p, which is not a GATA family member, inhibits Gln3p/Gat1p from functioning in the presence of good nitrogen sources. We show that NCR-sensitive *DAL80* transcription can be influenced by the relative levels of *GAT1* and *URE2* expression. NCR, normally observed with ammonia or glutamine, is severely diminished when Gat1p is overproduced, and this inhibition is overcome by simultaneously increasing *URE2* expression. Further, overproduction of Ure2p nearly eliminates NCR-sensitive transcription under derepressive growth conditions, *i.e.* with proline as the sole nitrogen source. Enhanced green fluorescent protein-Gat1p is nuclear when Gat1p-dependent transcription is high and cytoplasmic when it is inhibited by overproduction of Ure2p.

Two complementary modes of regulation are employed by *Saccharomyces cerevisiae* to achieve selective utilization of “good” nitrogen sources (ammonia, glutamine or asparagine) in preference to “poor” ones (proline), a process designated nitrogen catabolite repression (NCR)<sup>1</sup> (1–3). Both depend upon NCR-sensitive transcription being mediated through UAS<sub>NTR</sub> elements, containing GATAA sequences at their cores (4), and four members of the GATA-binding family of transcription factors, Gln3p, Gat1p/Nil1p, Dal80p, and Deh1p/Gzf3p/Nil2p (3, 5–12). The preeminent mode of regulation is that exerted by Ure2p, which inhibits the ability of the GATA activators, Gln3p and Gat1p, to function during times of nitrogen excess (3, 13, 14); *ure2* mutants become insensitive to NCR (15, 16). The second mode, whose function we consider to be one of fine tuning, is proposed to depend upon the GATA repressors Dal80p and Deh1p competing with Gln3p and Gat1p for binding to their DNA targets (13, 17).

\*This work was supported by National Institutes of Health Grant GM-35642. The costs of publication of this article were defrayed in part by the payment of page charges. This article must therefore be hereby marked “advertisement” in accordance with 18 U.S.C. Section 1734 solely to indicate this fact.

© 2000 by The American Society for Biochemistry and Molecular Biology, Inc.

<sup>‡</sup>To whom correspondence should be addressed. Tel.: 901-448-6175; Fax: 901-448-8462; tcooper@utmem.edu..

<sup>1</sup>The abbreviations used are: NCR, nitrogen catabolite repression; PCR, polymerase chain reaction; kb, kilobase(s); EGFP, enhanced green fluorescent protein.

Success of the regulatory mechanism hypothesized above requires the relative amounts of Gln3p, Gat1p, Dal80-p, and Deh1p to be rigorously and finely controlled. Such fine control has been proposed to be achieved through autogenous and cross-regulation of GATA factor production (6, 11), a view supported by (i) the presence of multiple UAS<sub>NTR</sub> elements situated upstream of the *DAL80*, *DEH1*, and *GAT1* genes and (ii) effects of *gln3*, *gat1*, *dal80:hisG*, and *deh1* mutations on expression of the three genes (3, 11, 12). Although the model fits existing data, its central tenant has not been tested experimentally, *i.e.* that expression of one GATA factor, *GAT1*, influences expression of another, *DAL80*.

The purpose of this work was to test the above proposal by determining the effects of varying *GAT1* expression on that of *DAL80*. The data obtained demonstrate that *DAL80* expression is tightly linked to that of *GAT1* and furthermore that NCR can be tightly linked to the relative production of Gat1p and Ure2p, *i.e.* that changing the relative levels of *GAT1* and *URE2* expression concomitantly changes the sensitivity of *DAL80* expression to NCR. We also find that the intracellular localization of EGFP-Gat1p is influenced by the levels of *GAT1* and *URE2* expression. When Gat1p-dependent transcription is high, EGFP-Gat1p is predominantly nuclear, whereas when it is inhibited by overproduction of Ure2p, Gat1p is cytoplasmic.

## MATERIALS AND METHODS

### Strains and Culture Conditions

The strains used are: TCY1 (*Mata lys2 ura3*), TCY5 (*Mata lys2 ura3 trp1:hisG*), TCY29 (*Mata lys2 ura3 trp1:hisG dal80:hisG*), TCY46 (*Mata lys2 ura3 trp1:hisG GAL1,10-GAT1*), TCY48 (*Mata lys2 ura3 trp1:hisG dal80:hisG GAL1,10-GAT1*), TCY57 (*Mata lys2 ura3 trp1:hisG leu2:hisG GAL1,10-URE2*), TCY60 (*Mata lys2 ura3 trp1:hisG leu2:hisG dal80:hisG GAL1,10-GAT1 GAL1,10-URE2*), RRJ715 (*Mata, lys2, ura3, his3, gat1:hisG*), RTC57 (*Mata, lys2, trp1, his3, ura3, URE2-GAL1-10*), and GYC86 (*Mata, his3, leu2, trp1, ura3/Mata, his3, leu2, trp1, ura3*). Minimal medium was 0.17% YNB without amino acids or (NH<sub>4</sub>)<sub>2</sub>SO<sub>4</sub> (Difco) with indicated carbon and nitrogen sources and auxotrophic requirements.

### Northern Blot and $\beta$ -Galactosidase Analyses

Yeast cultures for RNA analysis (see Figs. 2 and 4A) were grown in minimal proline galactose (2%) medium with glucose added to the final concentration indicated in the figure. For Fig. 4C, RRJ715, RRJ715/pRA27, and RTCY57/pRA27 were grown to  $A_{600\text{ nm}} = 0.3\text{--}0.4$  in Wickerham's minimal ammonia medium. RTCY57/pRA27 was washed and transferred to Wickerham's galactose medium for induction of URE2 (3 h). Total RNA was isolated (18, 19), resolved on formaldehyde-agarose gels, and transferred to Gene Screen Plus nylon 66 membranes (NEN Life Science Products) using 6 $\times$  SSC as the buffer. Random priming was used to label PCR product or DNA fragment probes. Hybridization was in 50% formamide, 1 M NaCl, 1% SDS (42  $^{\circ}$ C, 17–20 h). Blots were washed twice each in 2 $\times$  SSC at 25  $^{\circ}$ C, 2 $\times$  SSC + 1% SDS at 65  $^{\circ}$ C and 0.1 $\times$  SSC at 25  $^{\circ}$ C or as described (19).  $\beta$ -Galactosidase assays were based on 25 ml of culture. For *GAL1,10-GAT1-lacZ* or

*GAL1,10-URE2-lacZ* expression, freshly inoculated cultures (glucose ammonia medium) were grown overnight to a cell density of  $A_{600\text{ nm}} = 0.4\text{--}0.8$ .

### **GAL1,10-GAT1, and GAL1,10-URE2 Strains**

GAL1,10-GAT1 and *GAL1,10-URE2* fusion fragments were used to replace genomic *GAT1* and *URE2*. For *GAT1*, the 0.8-kb *SalI-XhoI* promoter fragment was cloned into pBSKS(+) (Stratagene) yielding pTSC613. The 0.8-kb *ApaI-SalI* *GAT1* fragment of pTSC613 was cloned into pLitmus38 yielding pTSC614. pTSC614 was digested with *BsgI*, and the backbone was isolated, deleting the 0.3-kb *GAT1 BsgI* fragment containing clustered GATAs. A blunt-ended polylinker (*BsrGI* to *MfeI*) from pLitmus38 was cloned into the *BsgI* site of the plasmid backbone, following Klenow treatment of the linearized DNA, yielding pTSC620. A Klenow-treated, *EcoRI* TRP1 fragment from YRp7 was digested with *PstI* and cloned into pTSC620 digested with *HindIII*, treated with Klenow, and then digested with *PstI*, yielding pTSC627. The *GAL1,10* promoter fragment was generated by Pwo PCR with oligonucleotide primers, 5'-GATCGCCGGCCCTTCTCTTTGGAACCTTCAGTAAT-3' and 5'-GATCGCCGGCTCGCTGATTAATTACCCAGAA-3', and pEG(KG) (20) as template. The PCR product was digested with *NgoMI* and cloned into pTSC627 partially digested with *NgoMI*. Restriction site analysis and DNA sequencing (*GAL1,10-GAT1* junction) confirmed the resulting construct, pTSC645. The *SalI-XhoI* fragment of pTSC645 was purified and used to transform relevant host strains.

The 1.1-kb *SalI-XhoI* *URE2* fragment from pRD17 (21) was cloned into pLitmus38, yielding pTSC638. The *BsrGI-XhoI* fragment of pTSC638 (containing 170 bp of the *URE2* promoter) was deleted and replaced by a PCR-generated *GAL1,10* promoter fragment (primers: 5'-CCGCTCGAGCCGAAGGAAGACTCTCCTCCG-3' and 5'-CGCTCTACAGACGTTAAAGTATAGAGGTAT-3', template, pEG(KG) (20)). Because the *URE2* promoter lacks a TATA box, the above PCR product included the *GAL1,10* TATA box and transcription start site(s) (22). The *BsrGI-XhoI* *GAL1,10* promoter fragment was ligated into the backbone of pTSC638, yielding pTSC650. A *SalI-XhoI* *LEU2* fragment (2) was then cloned into the unique *XhoI* site of pTSC650 yielding pTSC657. The *SalI-XhoI* and *SalI-ApaI* fragments of pTSC645 and pTSC657, respectively, were purified and used to transform the relevant strains. Integrants were verified by Southern blot analysis using multiple restriction endonucleases (data not shown).

### **GAL1,10-GAT1-lacZ, GAL1,10-URE2-lacZ, and GAL1,10-DAL80-lacZ Plasmids**

A *BamHI* oligonucleotide (10-mer) was ligated into *GAT1* pTSC645 digested with *XhoI* and treated with Klenow polymerase. The 0.9-kb *XbaI-BamHI* fragment containing the 5' end of *TRP1*, *GAL1,10 UAS* and the 5' end of *GAT1* (to position +193) was isolated and ligated into plasmid pHP41 (23) yielding pTSC666 (Fig. 1). For *GAL1,10-URE2*, a *BamHI* oligonucleotide (10-mer) was ligated onto *EagI*-digested, Klenow-treated pTSC657. The 0.7-kb *XhoI-BamHI* fragment (containing the *GAL1,10 UAS* and the 5' end of *URE2* to position +103) was ligated into pHP41 treated with *SalI* and *BamHI*, yielding pTSC668 (Fig. 1). For *GAL1,10-DAL80*, the 0.9-kb *Asp718-PvuII* fragment from pTSC674 was cloned into Litmus 28 to yield pTSC678. A *BamHI* oligonucleotide (10-mer) was ligated onto the blunt ends of pTSC678 digested with *PvuII*. The 0.9-kb *XbaI-BamHI* fragment

from this plasmid (containing the 3' end of *HIS3*, *GALI,10 UAS* and *DAL80* 5' end to position +46) was isolated and ligated into pHP41, yielding pTSC679 (Fig. 1).

### **EGFP-GAT1 pRA27 Was Constructed by Cloning a 1.7-kb NdeI**

*HindIII* *GAT1* fragment from pRR351 into pRMS2 (pADH1-EGFP, a 2  $\mu$  plasmid carrying a *HIS3* marker) allowing constitutive overexpression of *EGFP-GAT1* (24). All fusion junctions were sequenced to ensure they were in frame.

### **Fluorescence Microscopy**

Cytological experiments were performed as described elsewhere (25). The distribution of fluorescent material was the same whether cells were grown in Wickerham's or YNB minimal medium.

## **RESULTS**

### **GAT1 Expression under Control of the GAL1,10 Promoter**

Dissecting the regulatory relationships of the GATA transcription factors is hampered by their extensive autogenous- and cross-regulation (11, 12). To overcome this, we replaced the genomic *GAT1* promoter with a *GALI,10* fragment (*UAS<sub>GAL</sub>*), thereby removing *GAT1* expression from nitrogen and GATA factor control and placing it under galactose regulation. Because our experiments depended upon the transcription profile of the *GALI,10-GAT1* construct, we measured steady-state levels of *GAT1*-specific mRNA following three different glucose additions to the medium. *GAT1* mRNA increased as glucose decreased (Fig. 2A). Next, we substituted the *lacZ* open reading frame for the *GAT1* open reading frame in *CEN*-based *GALI,10-GAT1* pTSC666, measured  $\beta$ -galactosidase production under conditions similar to those in Fig. 2A, and found  $\beta$ -galactosidase activity decreased as the amount of glucose added to the medium increased (Fig. 2B). The inverse of the glucose addition was plotted on the abscissa throughout this work to facilitate visualization of the effects of *GALI,10* driven *GAT1* or *URE2* expression. As expected, *GALI,10-GAT1* expression is NCR-insensitive (Fig. 2B). In fact, *GALI,10-GAT1-lacZ* expression is 2- and 4-fold higher, respectively, with glutamine and ammonia compared with proline. This effect probably derives from ammonia and glutamine being significantly better nitrogen sources than proline and hence supporting higher synthetic capacities (26).

### **DAL80 Expression Is Strongly Influenced by the Level of GAT1 Expression**

A predicted consequence of the cross-regulation model of GATA factor control (11) is that the level of *GAT1* expression influences *DAL80* expression. We tested this prediction using a *DAL80-lacZ* reporter. We recognized from the outset that interpretation of our results could be compromised by: (i) down-regulation of *DAL80-lacZ* expression by Dal80p derived from the genomic *DAL80* gene responding to increased Gat1p (6) and (ii) secondary effects of growing cells with galactose as carbon source. We eliminated the first complication by performing our experiments in *dal80:hisG* disruption strain TCY48. To evaluate the second potential complication, we compared  $\beta$ -galactosidase production in wild type (TCY5) and *dal80:hisG* disruption (TCY29) strains transformed using *DAL80-lacZ*

pTSC572. The only difference in the *DAL80-lacZ* expression profile was a 20–30% decrease with galactose as carbon source (Fig. 2C), a relatively modest effect relative to that of NCR.

With the experimental system established, we determined the effect of varying *GATI* expression on *DAL80-lacZ* expression in TCY48. As the glucose concentration decreased (*GAT1* expression increased), *DAL80-lacZ* expression increased (Fig. 3). In addition to the *DAL80* expression expected when proline was provided as nitrogen source, increasing *GATI* expression unexpectedly increased *DAL80-lacZ* expression with ammonia and glutamine as nitrogen sources as well (Fig. 3). To place this result in perspective, *DAL80-lacZ* expression with ammonia as nitrogen source in Fig. 3 (3,969 units) is about 300-fold greater than normal (glutamine, 12 units) (11). In short, increasing *GATI* expression overcomes the repressive effects of preferred nitrogen sources on *DAL80-lacZ* expression.

### Increased URE2 Expression Suppresses the Effects of High Level GAT1 Expression

The current model of NCR proposes that the binding of Ure2p to Gln3p inhibits its ability to function as a transcriptional activator (27). Because Ure2p also regulates Gat1p-dependent NCR-sensitive transcription (9), we determined whether increasing *URE2* and *GATI* expression simultaneously would inhibit the ability of *GATI* to suppress the NCR sensitivity of *DAL80-lacZ* expression. Because the *GALI,10-URE2* construct could not be made in exactly the same way as *GALI,10-GATI*, we first determined whether the overall *GALI,10-URE2* transcription profile was similar to that of *GALI,10-GATI* (Fig. 2). Fig. 4 (A and B) shows that it was, except for a modest decrease in  $\beta$ -galactosidase production at the highest levels of *URE2* expression; the reason for this decrease is unknown. We found that increasing *URE2* and *GATI* expression together (Fig. 5A, *solid lines*) dramatically suppressed the ability of *GAT1* overexpression (Fig. 5A, *dotted lines*) to support high level *DAL80-lacZ* expression with proline or ammonia as nitrogen source. Moreover, *DAL80-lacZ* expression with *GATI* and *URE2* both overexpressed was fully NCR-sensitive. These data show that high level *URE2* expression neutralizes the effects of overexpressing *GATI*. Furthermore, increasing *GALI,10-URE2* expression (in TCY57) abrogated the need of an excess nitrogen “signal,” *i.e.* as *URE2* expression increased in a culture provided with a nonrepressive nitrogen source (proline),  $\beta$ -galactosidase production (*DAL80-lacZ* expression) correspondingly decreased (Fig. 5B).

### Gat1p Appears in the Nucleus Only When There Is Gat1p-dependent Transcription

We previously showed a correlation between intracellular distribution of a GATA factor, Gln3p, and NCR-sensitive gene expression.<sup>2</sup> Therefore, we wanted to determine whether *DAL80* expression correlated with the localization of Gat1p. We constructed *ADHI-EGFP-GATI* pRA27 and used it to transform *gat1* (RRJ715) cells. In this strain Ure2p is produced at wild type levels, and *GATI* is constitutively overexpressed. *DAL80* was highly expressed in the transformants (Fig. 4C, *lane B*). When the experiment was repeated in strain RTCY57, which overproduces Ure2p, no *DAL80* expression was detected (Fig. 4C), confirming the observations in Fig. 5A. When similarly prepared cultures were viewed microscopically, EGFP-Gat1p fluorescence was predominantly nuclear when *URE2* was

<sup>2</sup>Cox, K. H., Rai, R., Distler, M., Daugherty, J. R., Coffman, J., and Cooper, T. G. (2000) *J. Biol. Chem.*, in press.

expressed at wild type levels (Fig. 6, *K–Y*) and co-localized with DAPI-stained material (panels *a–i*). On the other hand, no nuclear localization was observed when *URE2* was overexpressed and *DAL80* expression was inhibited (Fig. 4C). Fluorescence rather appeared in the cytoplasm as punctate spots (Fig. 6, *A–J*) similar to those observed when cultures were transformed with *GFP-URE2* pNVS22 (data not shown, but it appears as in Fig. 9 of Cox *et al.*<sup>2</sup> and as reported earlier by Wickner's laboratory (28)).

## DISCUSSION

The cross-regulation model (11) of GATA factor regulation in *S. cerevisiae* posits that *GATI* expression directly regulates the level of *DAL80* expression and hence Dal80p production. To test this prediction we circumvented the complex normal cross-regulation observed among GATA factor genes and their products by substituting *GALI,10* for the *GATI* and/or *URE2* promoters and demonstrated that we could obtain cultures containing differing amounts of *GATI* and *URE2* expression and mRNA, which implies they also produced differing amounts of Gat1p and Ure2p. Using this experimental system, we demonstrated that *DAL80-lacZ* expression (i) depended upon *GATI* expression, (ii) became significantly insensitive to NCR when *GATI* was overexpressed, and (iii) regained NCR sensitivity when *URE2* was simultaneously overexpressed with *GATI*.

To further evaluate the relationship between *GATI* and *DAL80* expression, we plotted *GALI,10-GATI-lacZ* expression data from Fig. 2B as a function of *DAL80-lacZ* expression (Fig. 3). A linear relationship exists at all but the highest levels of *GATI* expression with proline as nitrogen source (Fig. 7). This linear relationship is not observed with glutamine as nitrogen source until *GALI,10-GATI-lacZ* expression was much higher (Fig. 7B). A similar relationship was also observed with ammonia (Fig. 7C). These data are expected of a situation in which functional Gat1p is “titrating” an inhibitor with ammonia or glutamine as nitrogen sources, and increased *DAL80-lacZ* expression is not observed until Gat1p exceeds a critical level, thereafter overcoming inhibition. Data in Fig. 5 suggest that the molecule Gat1p is likely titrating is Ure2p, because the effects of increased *GATI* expression are suppressed when *URE2* expression is simultaneously increased. These results are consistent with the possibility that Gat1p forms a complex with Ure2p as has been suggested for Gln3p (27).

Microscopic evidence extended the relationship between Gat1p and Ure2p by demonstrating that Gat1p localizes predominantly to the nucleus when Gat1p-dependent transcription is occurring and is cytoplasmic when this transcription is inhibited by overproduction of Ure2p. In other words, Ure2p prevents Gat1p from reaching its physiological target, the GATA elements in NCR-sensitive gene promoters. A similar conclusion was reached for control of Gln3p operation from analysis of *CAN1* expression.<sup>2</sup>

Taken together, the data lead us to suggest that expression of GATA factor-regulated genes depends upon binding of the transcriptional activators Gln3p and Gat1p to their promoter targets and that once bound the activators are able to mediate transcriptional activation and gene expression. Although a negative observation, the finding that Gln3p tethered to DNA by LexAp mediates reporter gene transcription that exhibits little if any NCR-sensitive

control (29) is consistent with this proposal. From this perspective, GATA factor regulation is achieved by regulating its binding to its promoter targets. At a coarse level this most likely occurs by regulating Gln3p and Gat1p access to the nucleus that is regulated by Ure2p. At a fine level, once the transcriptional activators have gained access to the nucleus, their overall level of operation is regulated by competition with the transcriptional repressors Dal80p and Deh1p for DNA binding. The fluidity and fine nature of the overall regulation is then achieved by the fact that production of three of the four GATA factors is autogenously and cross-regulated.

Data in Fig. 5B highlight an important characteristic of Ure2p participation in the NCR regulatory cascade. Increasing the intracellular concentration of Ure2p appears to eliminate the need for the physiological signal that intracellular nitrogen is in excess. This observation is consistent with the ideas that: (i) Ure2p exists as an inactive form that is activated in response to a signal indicating nitrogen excess and (ii) Ure2p exists in an active form that is inactivated in response to a signal indicating nitrogen limitation. By this reasoning, signal(s) generated in response to intracellular nitrogen excess or limitation can be circumvented by increasing the concentration of Ure2p or neutralizing negative control exerted by Ure2p by increasing the concentration of at least one of the GATA activators, in this case Gat1p. The simplest basis for such concentration-dependent control is protein-protein complex formation among the constituents of the regulatory circuit.

As this manuscript was being written, four reports simultaneously appeared reaching conclusions to which ours are both similar and complementary (30–33). Although there is not full agreement on the mechanistic details, all propose that Ure2p complexes with one form or another of Gln3p, thereby preventing its entry into the nucleus when cells are grown in rich medium, and one of them demonstrated the proposed Gln3p nuclear and cytoplasmic localization (30). A similar model was proposed for Gat1p, although the investigators were unable to show any interaction between Gat1p and Ure2p. Our work points to such an interaction and contributes to filling this missing link in the proposed models.

## Acknowledgments

We thank Dr. R. Rai for pRR351 (T7-7-GAT1), Tim Higgins for preparing the artwork, and the UT Yeast Group for suggested improvements to the manuscript.

## REFERENCES

1. Cooper, TG. The Molecular Biology of the Yeast *Saccharomyces*: Metabolism and Gene Expression. Strathern, JN.; Jones, EW.; Broach, J., editors. Cold Spring Harbor Laboratory, Cold Spring Harbor, NY: 1982. p. 39-99.
2. Wiame J-M, Grenson M, Arst H. *Adv. Microb. Physiol.* 1985; 26:1–87. [PubMed: 2869649]
3. ter Schure EG, van Riel NA, Verrips CT. *FEMS Microbiol. Rev.* 2000; 24:67–83. [PubMed: 10640599]
4. Bysani N, Daugherty JR, Cooper TG. *J. Bacteriol.* 1991; 173:4977–4982. [PubMed: 1860815]
5. Chisholm G, Cooper TG. *Mol. Cell. Biol.* 1982; 2:1088–1095. [PubMed: 6757722]
6. Cunningham TS, Cooper TG. *Mol. Cell. Biol.* 1991; 11:6205–6215. [PubMed: 1944286]
7. Mitchell AP, Magasanik B. *Mol. Cell. Biol.* 1984; 4:2758–2766. [PubMed: 6152012]
8. Minehart PL, Magasanik B. *Mol. Cell. Biol.* 1991; 11:6216–6228. [PubMed: 1682800]

9. Coffman JA, Rai R, Cunningham T, Svetlov V, Cooper TG. *Mol. Cell. Biol.* 1996; 16:847–858. [PubMed: 8622686]
10. Stanbrough M, Rowen DW, Magasanik B. *Proc. Natl. Acad. Sci. U. S. A.* 1995; 92:9450–9454. [PubMed: 7568152]
11. Coffman JA, Rai R, Loprete DM, Cunningham T, Svetlov V, Cooper TG. *J. Bacteriol.* 1997; 179:3416–3429. [PubMed: 9171383]
12. Soussi-Boudekou S, Vissers S, Urrestarazu A, Jauniaux J-C, Andre B. *Mol. Microbiol.* 1997; 23:1157–1168. [PubMed: 9106207]
13. Cooper, TG. *Mycota III*. Marzluf, G.; Bambrel, R., editors. Springer-Verlag; Berlin: 1994. p. 139-169.
14. Courchesne WE, Magasanik B. *J. Bacteriol.* 1988; 170:708–713. [PubMed: 2892826]
15. Drillien R, Aigle M, Lacroute F. *Biochem. Biophys. Res. Commun.* 1973; 53:367–372. [PubMed: 4146147]
16. Drillien R, Lacroute F. *J. Bacteriol.* 1972; 109:203–208. [PubMed: 4550662]
17. Cunningham TS, Dorrington RA, Cooper TG. *J. Bacteriol.* 1994; 176:4718–4725. [PubMed: 8045902]
18. Daugherty JR, Rai R, ElBerry HM, Cooper TG. *J. Bacteriol.* 1993; 175:64–73. [PubMed: 8416910]
19. Cox K, Pinchak AB, Cooper TG. *Yeast.* 1999; 15:703–713. [PubMed: 10392447]
20. Mitchell DA, Marshall TK, Deschenes RJ. *Yeast.* 1993; 9:715–723. [PubMed: 8368005]
21. Coffman JA, El Berry HM, Cooper TG. *J. Bacteriol.* 1994; 176:7476–7483. [PubMed: 8002570]
22. Johnston M, Davis R. *Mol. Cell. Biol.* 1984; 4:1440–1448. [PubMed: 6092912]
23. Park H-D, Luche RM, Cooper TG. *Nucleic Acids Res.* 1992; 20:1909–1915. [PubMed: 1579492]
24. Christianson TW, Sikorski RS, Dante M, Shero JH, Hieter P. *Gene (Amst.)*. 1992; 110:119–122. [PubMed: 1544568]
25. Scott S, Dorrington R, Svetlov V, Beeser AE, Distler M, Cooper TG. *J. Biol. Chem.* 2000; 275:7198–7204. [PubMed: 10702289]
26. Kovari L, Sumrada R, Kovari I, Cooper TG. *Cell Biol.* 1990; 10:5087–5097.
27. Blinder D, Coschigano P, Magasanik B. *J. Bacteriol.* 1996; 178:4734–4736. [PubMed: 8755910]
28. Edskes HK, Gray V, T. Wickner RB. *Proc. Natl. Acad. Sci. U. S. A.* 1999; 96:1498–1503. [PubMed: 9990052]
29. Cunningham TS, Svetlov V, Rai R, Cooper TG. *J. Bacteriol.* 1995; 178:3470–3479. [PubMed: 8655543]
30. Beck T, Hall MN. *Nature.* 1999; 402:689–692. [PubMed: 10604478]
31. Cardenas ME, Cutler NS, Lorenz M, Di Como CJ, Heitman J. *Genes Dev.* 1999; 13:3271–3279. [PubMed: 10617575]
32. Hardwick JS, Kuruvilla FG, Tong JK, Shamji AF, Schreiber S. *Proc. Natl. Acad. Sci. U. S. A.* 1999; 96:14866–14870. [PubMed: 10611304]
33. Hardwick JS, Tong JK, Schreiber SL. *Nature Genetics.* 1999; 23:49.



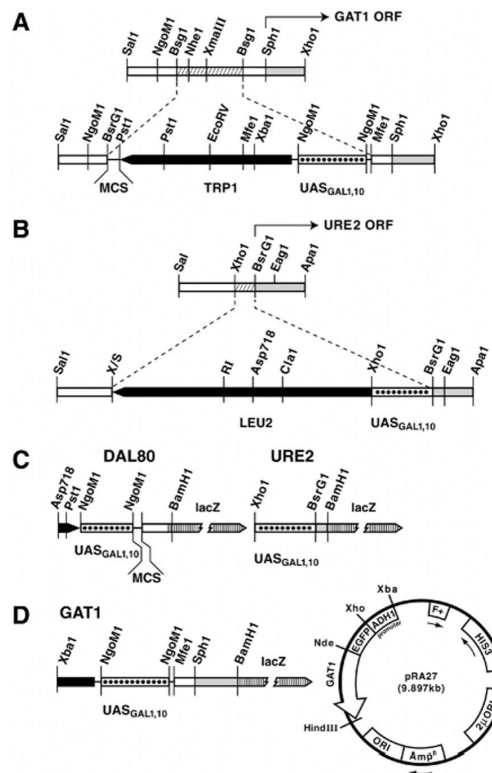


**Fig. 1. Fusion plasmids and genes used in this work**

The native *GAT1* and *URE2* genomic regions are shown before and after promoter substitutions have occurred. *Open bars*, native sequences; *hatched bars*, deleted sequences; *filled bars*, selected gene; *dotted bars*, *GAL1,10* regulatory sequences; *shaded bars*, open reading frames; *vertically striped bars*, *lacZ*. *GAT1* and *URE2* open reading frames begin at the *SphI* and near the *BsrGI* sites, respectively. *X/S* is a *SalI*-*XhoI* junction.

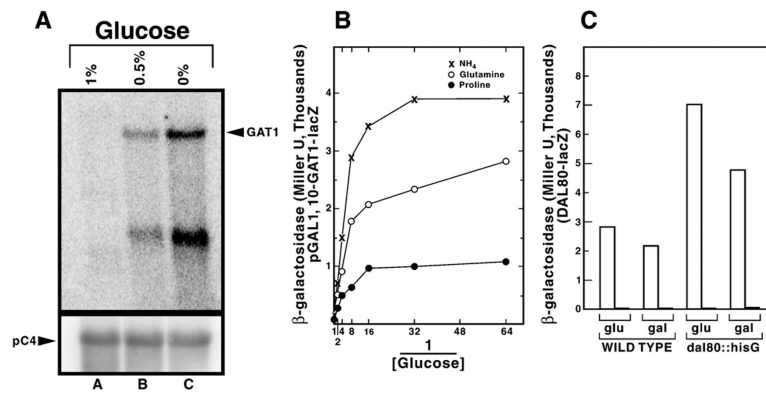


**Fig. 2. *GAL1,10-GAT1* expression profile measured by Northern blot analysis (A) and by  $\beta$ -galactosidase production supported by *GAL1,10-GAT1-lacZ* fusion plasmid (B)**

Total RNA (20  $\mu$ g/lane) was prepared from *GAL1,10-GAT1* strain TCY46 grown in minimal galactose proline medium plus the indicated amount of added glucose. [<sup>32</sup>P]dCTP-labeled probes were synthesized from the internal 1-kb *SphI-StuI* fragment of *GAT1* and pC4 (33).  $\beta$ -Galactosidase production from pTSC666 (in strain TCY48) was measured following addition of various amounts of glucose (final concentration was 0, 0.016, 0.032, 0.063, 0.125, 0.25, 0.5 or 1%) to minimal galactose (2%) medium containing proline (●), glutamine (○), or ammonium sulfate (x) as nitrogen source. C, *DAL80-lacZ* expression in wild type and *dal80* strains grown in different carbon and nitrogen sources.  $\beta$ -Galactosidase activity supported by plasmid pTSC572 was assayed in wild type (TCY5) or *dal80::hisG* (TCY29) strains. *Open* and *filled bars* denote proline and asparagine, respectively, as the nitrogen source. Glucose (*glu*) or galactose (*gal*) was used as the sole carbon source.

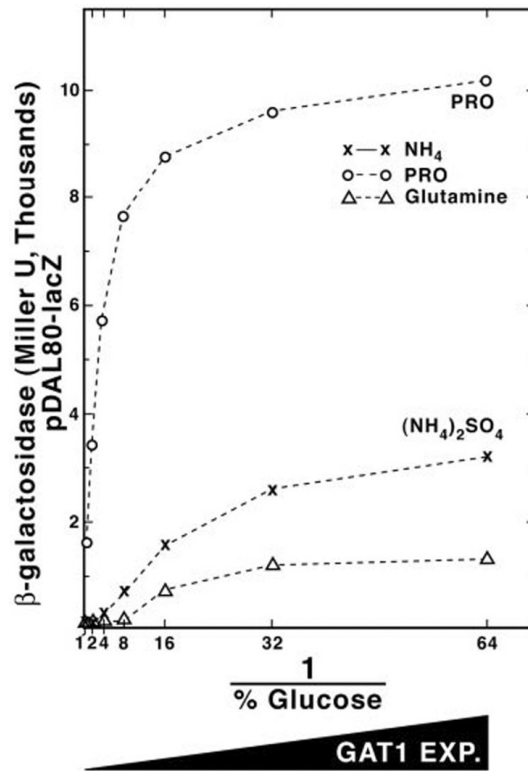


**Fig. 3. *DAL80-lacZ* expression observed at various levels of *GAT1* expression**  
 $\beta$ -Galactosidase production, supported by *DAL80-lacZ* pTSC572, was measured in a transformant of *GAL1,10-GAT1* strain TCY48 growing in minimal medium containing proline (○), ammonium sulfate (×), or glutamine (△) as sole nitrogen source. *GAT1 EXP.* indicates *GAT1* expression.

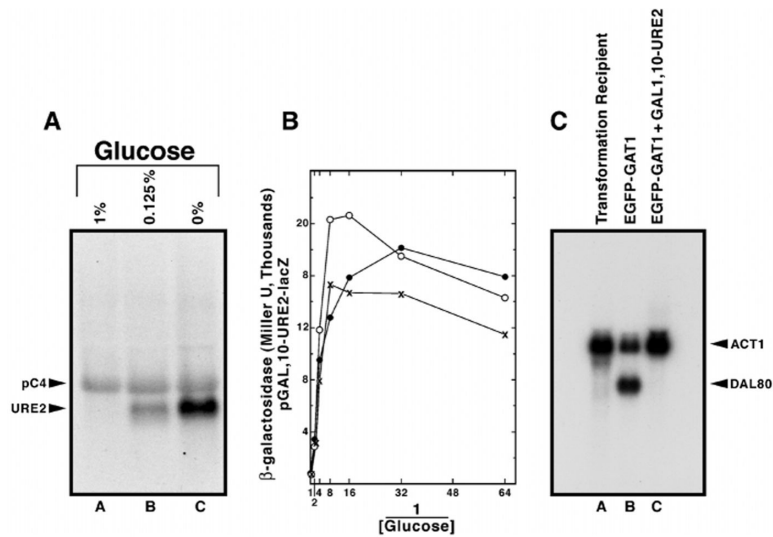


**Fig. 4. *GAL1,10-URE2* expression profile measured by Northern blot analysis (A) and by  $\beta$ -galactosidase production supported by *GAL1,10-URE2-lacZ* fusion (B)**

Details of the Northern blot analysis were as in Fig. 2 using strain TCY57 was grown in galactose-proline minimal medium with the indicated amount of glucose added.  $^{32}$ P-Labeled probes were synthesized from the 0.45-kb *BsrGI-ApaI* fragment from *URE2* and yeast pC4  $\beta$ -Galactosidase production from pTSC668 (in strain TCY1) was measured as in Fig. 2. C, Northern blot analysis of total RNA (9  $\mu$ g/lane) from strain RRJ715, untransformed (lane A) or transformed pRA27 (lane B), and strain RTCY57 transformed with pRA27 (lane C). Strains were grown in minimal glucose ammonia medium, and RTCY57 was additionally transferred to galactose ammonia medium and induced for 3 h prior to assay. Full-length *DAL80* and *ACT1* probes were used.

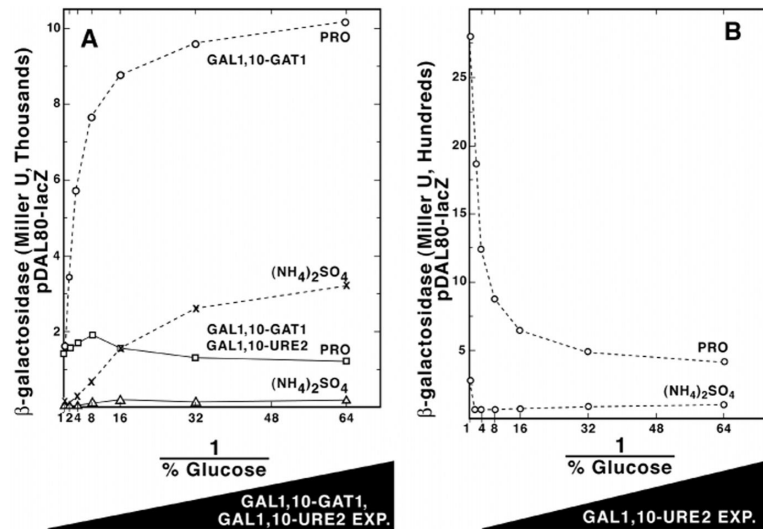


**Fig. 5.** A, expression of the *DAL80-lacZ* gene in strains expressing *GAT1* or *GAT1 1 URE2* at various levels. Strain TCY48 was grown with either proline (○) or ammonium sulfate (×) as sole nitrogen source in galactose minimal medium, to which was added the indicated amounts of glucose. Strain TCY60, containing plasmid pTSC572, was grown with either proline (□) or ammonium sulfate (△) as sole nitrogen source. B, *DAL80-lacZ* expression (from pTSC572) in strain TCY57 expressing *URE2* at various levels.

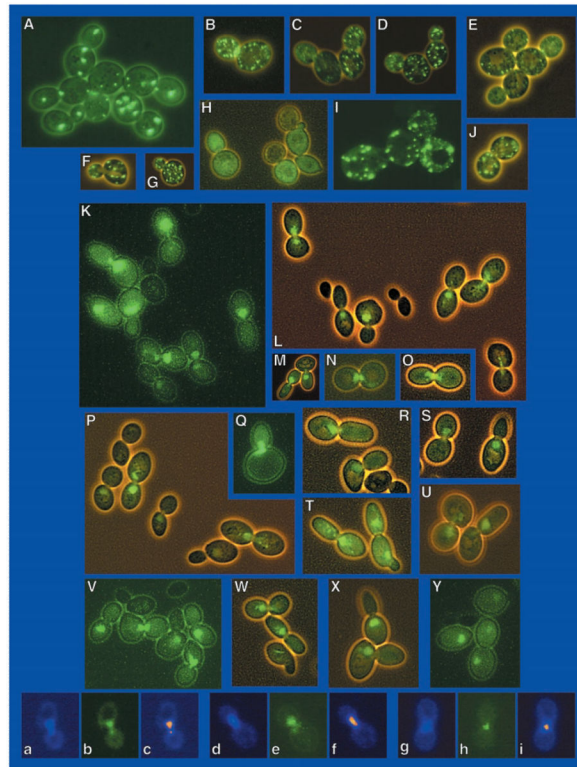


**Fig. 6.** A–J, ADH1-EGFP-GAT1 expressed in RTCY57 that overexpresses *GAL1,10-URE2*. K–Y, ADH1-EGFP-GAT1 expressed in wild type GYC86. Panels a, d, and g were stained with 4,6-diamidino-2-phenylindole; EGFP-GAT1p was visualized in panels b, e, and h. In panels c, f, and i, the 4,6-diamidino-2-phenylindole-positive material in panels a, d, and g was pseudocolored red, and the images were superimposed on those in panels b, e, and h.

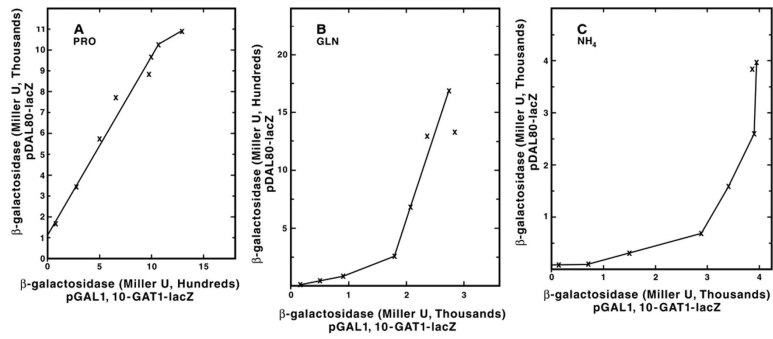


**Fig. 7. *DAL80-lacZ* expression plotted as a function of *GAT1-lacZ* expression in medium containing proline (A), glutamine (B), or ammonia (C) as sole nitrogen source**  
Data in this figure derive from Figs. 2B and 3.